J|A|C|S ARTICLES

Published on Web 05/14/2010

Insights into Initial Kinetic Nucleation of Gold Nanocrystals

Tao Yao,[†] Zhihu Sun,[†] Yuanyuan Li,[†] Zhiyun Pan,[†] He Wei,[‡] Yi Xie,*[,‡] Masaharu Nomura,[§] Yasuhiro Niwa,[§] Wensheng Yan,[†] Ziyu Wu,[†] Yong Jiang,[†] Qinghua Liu,[†] and Shiqiang Wei*[,†]

National Synchrotron Radiation Laboratory, University of Science and Technology of China, Hefei, Anhui 230029, People's Republic of China, Department of Nanomaterials and Nanochemistry, Hefei National Laboratory for Physical Sciences at Microscale, University of Science and Technology of China, Hefei 230026, People's Republic of China, and Photon Factory, Institute of Materials Structure Science, High Energy Accelerator Research Organization (KEK), Tsukuba, Ibaraki 305-0801, Japan

Received February 6, 2010; E-mail: sqwei@ustc.edu.cn; yxie@ustc.edu.cn

Abstract: Understanding the initial nucleation mechanism of monodisperse nanocrystals (NCs) during synthesis process is an important prerequisite to control the desired sizes and to manipulate the properties of nanoscale materials. The acquisition of information for the small nanocluster nucleation process, however, still remains challenging. Here, using a continuous-flow *in situ* X-ray absorption fine structure (XAFS) spectroscopy for time-resolved studies, we have clarified the initial kinetic nucleation of Au clusters under the grain size of 1 nm for the classical Au NCs synthesis via the reduction of $AuCl_4^-$ in aqueous solution. The *in situ* XAFS results present the experimental revelation of the formation of intermediate $Cl_3^-Au-AuCl_3^-$ dimer and the subsequent higher complexes 'Au_nCl_{n+x}' in the initial nucleation stage. We propose a kinetic three-step mechanism involving the initial nucleation, slow growth, and eventual coalescence for the Au NCs formation, which may be helpful for the synthesis of metallic nanomaterials.

Introduction

Noble-metallic nanocrystals (NCs) of controlled size and shape have attracted increasing research attention during the past decades due to their interesting dimension dependent optical, electronic, and catalytic properties.[1−3] Colloidal chemical synthetic methods involving the reduction of a precursor by various reducing agents at an elevated temperature in the presence of a polymeric stabilizer such as polyvinyl pyrrolidone (PVP) have been widely developed for the production of uniform Au NCs.[4,5] Recently, the nucleation mechanism of metallic NCs in solution have been a subject of the increasing study, but are still poorly understood due to the limitation of the conventional characterization methods.[6,7]

A number of approaches have been developed to address this technical challenge, both from experimental and theoretical points of view.[6,8−11] Theoretically, Frenkel et al.[8] and Bawendi et al.[9] have developed a simple and general model to simulate the nucleation rate and size evolution. Further computational studies need to be guided by more solid experimental evidence of nucleation event. *In situ* experimentation with a time-resolution represents the most likely means by which the key stages of dynamic processes in the NCs nucleation can be unraveled. Many *in situ* researches have been devoted to the studies on the NCs nucleation using various techniques such as SAXS/WAXS, UV−vis, and transmission electron microscopy (TEM).[10,11] For example, Abécassis et al.[10] have reported an *in situ* study on the nucleation and growth of Au NCs by using SAXS/WAXS and UV−vis spectroscopy. More recently, Alivisatos and co-workers[11] have successfully observed the growth trajectories of Pt NCs starting from the size of 2.2 nm in solution by *in situ* TEM.

These experimental methods are mainly utilized to study the growth process of NCs in a size larger than 1−2 nm; however, they could hardly provide effective information about the initial nucleation process from the atomic level. Currently, there are two pathways describing the generation of the initial nuclei of metal nanoclusters from the precursors.[5,6] One is the classical path of nucleation where metallic ions are fully reduced into the zerovalent atoms first and then aggregate into nuclei and grow into NCs.[12,13] The other is the formation of cluster

[†] National Synchrotron Radiation Laboratory, University of Science and Technology of China.

[‡] Hefei National Laboratory for Physical Sciences at Microscale, University of Science and Technology of China.

[§] High Energy Accelerator Research Organization (KEK).

(1) Sun, Y. G.; Xia, Y. N. *Science* **2002**, *298*, 2176.
(2) Habas, S. E.; Lee, H.; Radmilovic, V.; Somorjai, G. A.; Yang, P. *Nat. Mater.* **2007**, *6*, 692.
(3) Wang, C.; Hu, Y. J.; Lieber, C. M.; Sun, S. H. *J. Am. Chem. Soc.* **2008**, *130*, 8902.
(4) Park, J.; Joo, J.; Kwon, S. G.; Jang, Y.; Hyeon, T. *Angew. Chem., Int. Ed.* **2007**, *46*, 4630.
(5) Xia, Y.; Xiong, Y. J.; Lim, B.; Skrabalak, S. E. *Angew. Chem., Int. Ed.* **2009**, *48*, 60.
(6) Finney, E. E.; Finke, R. G. *J. Colloid Interface Sci.* **2008**, *317*, 351.
(7) Oxtoby, D. W. *Nature* **2000**, *406*, 464.
(8) Auer, S.; Frenkel, D. *Nature* **2001**, *409*, 1020.
(9) Rempel, J. Y.; Bawendi, M. G.; Jensen, K. F. *J. Am. Chem. Soc.* **2009**, *131*, 4479.
(10) Abecassis, B.; Testard, F.; Spalla, O.; Barboux, P. *Nano Lett.* **2007**, *7*, 1723.
(11) Zheng, H. M.; Smith, R. K.; Jun, Y. W.; Kisielowski, C.; Dahmen, U.; Alivisatos, A. P. *Science* **2009**, *324*, 1309.
(12) LaMer, V. K.; Dinegar, R. H. *J. Am. Chem. Soc.* **1950**, *72*, 4847.

 10.1021/ja101101d

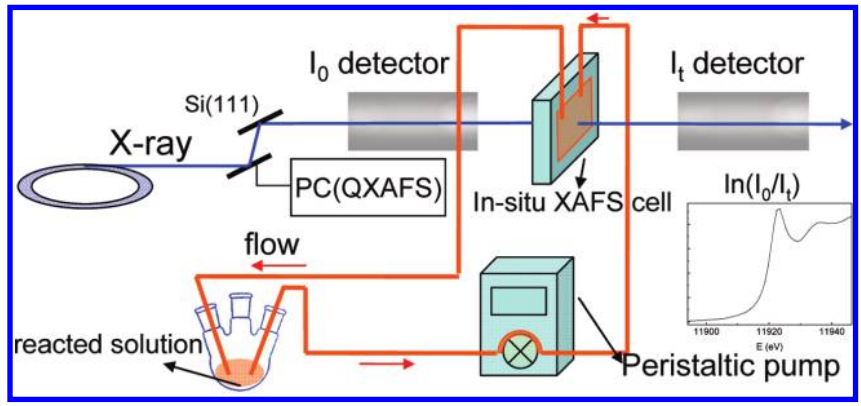

Figure 1. Schematic presentation of the experimental setup employed for *in situ* QXAFS measurements during the formation of Au NCs.

complex by unreduced metal species prior to full reduction to the metallic state.[14,15] We summarize these two pathways by the following equations:

$$\text{Path 1: } M^{x+} + xe \rightarrow M^0, \quad M^0 + M_n^0 \rightarrow M_{n+1}^0$$

$$\text{Path 2: } M^{x+} + e \rightarrow M^{(x-1)+}, \quad M^{(x-1)+} + M^{(x-1)+} \rightarrow M_2^{(2x-2)+}$$

Therefore, a technique sensitive to the temporal evolution around an atomic species is essential to fill the gap of the knowledge about the initial stage of NCs growth. Fortunately, due to the deep penetration of X-ray and atomic species identity, time-resolved *in situ* X-ray absorption fine structure (XAFS) spectroscopy is a powerful method to carry out a direct investigation for the local structural change during the reactive processes in a bulk or a solution system.[16−20]

Here, we report an *in situ* time-resolved XAFS technique with an atomic scale sensitivity to monitor the initial formation kinetics of Au NCs under the grain size of 1 nm. The developed time-resolved XAFS setup with continuous-flow mode is shown in Figure 1. This online characterization technique can enable us to detect the structural changes in the initial nucleation process of Au clusters without an additional sample preparation step. The synthesis of Au NCs was performed through the reduction of $HAuCl_4$ by citric acid in an aqueous surfactant solution (PVP). The use of citric acid as the reducing agent together with low reaction temperature has permitted us to study the moderate nucleation kinetics over relatively long period of a few hours. The reduction process can be monitored by the color changes in the solution from the initially transparent yellow to finally dark brown (see Figure S1, Supporting Information).

Experimental Section

Synthesis. Au nanocrystals were prepared by modifying the method of ref 5. Briefly, the aqueous solution containing 7.4 mM Auric acid ($HAuCl_4$), 28 mM citric acid, and 29 mM poly(vinyl pyrrolidone) (PVP) were mixed in a three-necked flask. The flask was connected with the *in situ* cell and the peristaltic pump through the microtubes. The reaction mixture was heated at 70 °C in air for 260 min with stirring.

Characterizations. At different reaction times, a small volume of liquid samples was extracted from the batch of reaction solution during the course of a reaction and spread as a droplet onto a copper grid for TEM measurements. The UV−vis absorption spectra were recorded on UV-2501PC/2550 spectrophotometer to detect the reduction of Au ions in the solutions.

In situ quick XAFS (QXAFS) measurements at Au L_{III}-edge were performed in transmission mode at NW10A station in PF-AR (Photon Factory Advanced Ring for Pulse X-ray, Japan) and U7C XAFS station in NSRL (National Synchrotron Radiation Laboratory, P.R. China). The storage ring of PF-AR was operated at 6.5 GeV with the maximum current of 450 mA. An approximate X-ray photon flux of 10^{11} photons s^{-1} was monochromatized using a Si(311) monochromator. The storage ring of NSRL was run at 0.8 GeV with the maximum current of 200 mA. In the QXAFS measurements, the Si(311) monochromator was moved continuously, so that quick measurement (less than several seconds to minutes) became possible. The reactive solution prepared by the procedure mentioned above was continuously circulated along the tubes by peristaltic pump during the acquisition of XAFS spectra and flowed into Teflon cell sealed with Kapton windows. The *in situ* Teflon cell has a path length in X-ray direction of about 5 mm. Because the static reacted vessel is not suitable for the *in situ* measurement directly, we used recirculation system instead to ensure that the samples at the spot were newly formed from the reacted solution to achieve *in situ* detection. The recirculation system also has additional advantages that it could avoid the precipitation of particles after a long time reaction and the possible influence of X-ray irradiation in XAFS measurements.[21,22] (see more detail in Supporting Information and Figure S2). The structural parameters were determined by a curve-fitting procedure in *R* space by using the FEFFIT program and USTCXAFS software packages.

Results and Discussion

Typical TEM images of gold NCs (Figure 2a) illustrate the formation of NCs with the reaction times. It should be noted that at the initial nucleation stage before 60 min, the NCs is difficult to be distinguished in the TEM field of view. Until 120 min, the typical Au NCs of about 2.5 nm can be observed clearly. Similarly, by using *in situ* TEM, Alivisatos et al. have traced the growth process of Pt NCs with the size of 3.4 nm

(13) Duff, D. G.; Edwards, P. P.; Johnson, B. F. G. *J. Phys. Chem.* **1995**, *99*, 15934.
(14) Henglein, A.; Giersig, M. *J. Phys. Chem. B* **2000**, *104*, 6767.
(15) Ciacchi, L. C.; Pompe, W.; De Vita, A. *J. Am. Chem. Soc.* **2001**, *123*, 7371.
(16) Wang, Q.; Hanson, J. C.; Frenkel, A. I. *J. Chem. Phys.* **2008**, *129*, 234502.
(17) Okumura, K.; Honma, T.; Hirayama, S.; Sanada, T.; Niwa, M. *J. Phys. Chem. C* **2008**, *112*, 16740.
(18) Hwang, B. J.; Chen, C. H.; Sarma, L. S.; Chen, J. M.; Wang, G. R.; Tang, M. T.; Liu, D. G.; Lee, J. F. *J. Phys. Chem. B* **2006**, *110*, 6475.
(19) Zhang, X. F.; Sun, Z. H.; Yan, W. S.; Wei, F.; Wei, S. Q. *Mater. Chem. Phys.* **2008**, *111*, 513.
(20) Yao, T.; Yan, W. S.; Sun, Z. H.; Pan, Z. Y.; He, B.; Jiang, Y.; Wei, H.; Nomura, M.; Xie, Y.; Xie, Y. N.; Hu, T. D.; Wei, S. Q. *J. Phys. Chem. C* **2009**, *113*, 3581.
(21) Mesu, J. G.; van der Eerden, A. M. J.; de Groot, F. M. F.; Weckhuysen, B. M. *J. Phys. Chem. B* **2005**, *109*, 4042.
(22) Mesu, J. G.; Beale, A. M.; de Groot, F. M. F.; Weckhuysen, B. M. *J. Phys. Chem. B* **2006**, *110*, 17671.

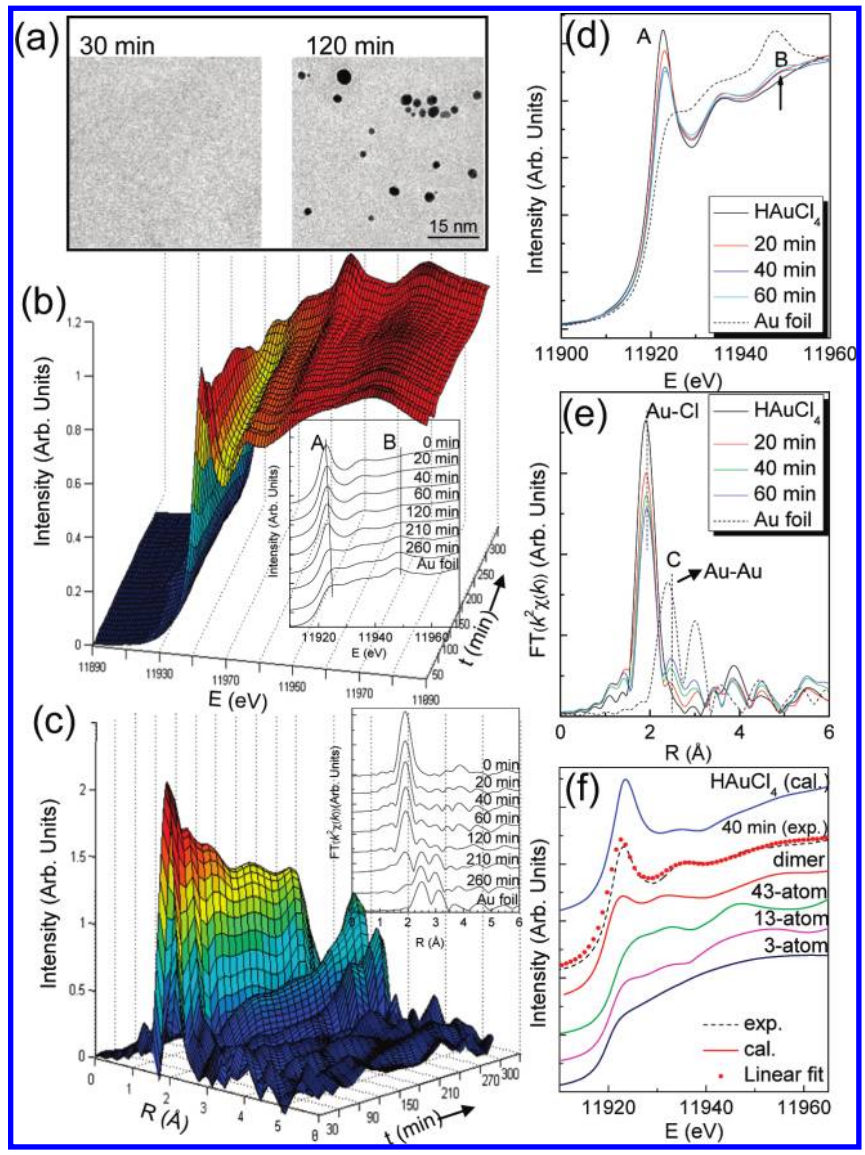

Figure 2. Dynamic nucleation and growth of Au NCs studied by TEM and *in situ* XAFS. (a) TEM images of Au NCs obtained at different times for 30 and 120 min. Time variations in normalized Au L_3-edge *in situ* XANES (b) and k^2-weighted EXAFS Fourier transforms (FTs) spectra (c). The insets show the typical Au L_3-edge XAFS spectra at different reaction time. For the purpose of investigating the nucleation process fairly, several typical data are compared in XANES (d) and the corresponding FTs (e) spectra. (f) XANES calculations for various Au clusters. The structural model of the naked Au_n^0 cluster adopts the most stable configurations. The dimer is assumed as the $Cl_3^-Au-AuCl_3^-$ model arises from two partially reduced $AuCl_3^-$ ions connected via Au−Au bond.

reduced by the electron beam.[11] No evident NCs could be found within the initial 10 s of reaction, while the NCs with the size of 2.2 nm appeared at 12 s. Up to date, however, there are few *in situ* studies reporting the observation of NCs with the size smaller than 2 nm, possibly because the nuclei formed in the initial stage are typically too small to be seen.

The *in situ* Au L_3-edge XANES and EXAFS spectra of Au colloidal solutions at sequential reaction times are shown in Figure 2b−e. As the reaction progressed, we can observe that the XANES spectra exhibit a clear decrease in intensity for the white line peak A (11922.5 eV) corresponding to a $2p_{3/2}$ to $5d_{5/2;3/2}$ dipole transition of Au atoms[23] and a slow increase for the peak B (11948.7 eV) in Figure 2b. The spectra of Fourier transforms (FTs) in Figure 2c directly demonstrate the local structure evolution around Au atoms. At the beginning, only a prominent peak at 1.90 Å ascribed to the Au−Cl bonds of $HAuCl_4$ is visible. With increasing reaction time, a peak C at 2.44 Å (uncalibration) attributed to the Au−Au bonds appears and its intensity is gradually enhanced. To peer into the structural evolution of the initial nucleation, we put more emphasis on the XAFS spectra during the reaction time of 0−60 min as shown in Figure 2d,e. At the reaction time of 20 min, the characteristic peak B marked by arrow already emerges and the white line peak A is lowered in intensity by just about $^1/_{10}$, which is different from the previous observations[24,25] that an induction period is needed before the onset of metal−metal bond signal. Also, the peak C of Au−Au bond can be observed. The results indicate that the partial reduction of $AuCl_4^-$ occurs with the formation of Au−Au bonds during the initial process. Hence, the nucleation of Au clusters with the particle size smaller than

(23) Zhang, P.; Sham, T. K. *Phys. Rev. Lett.* **2003**, *90*, 245502.
(24) Harada, M.; Einaga, H. *Langmuir* **2007**, *23*, 6536.
(25) Fernandez, A.; Caballero, A.; Gonzalezelipe, A. R.; Herrmann, J. M.; Dexpert, H.; Villain, F. *J. Phys. Chem.* **1995**, *99*, 3303.

1 nm at the initial stage can be well monitored by *in situ* XAFS. At the reaction time of 260 min, the XANES and the EXAFS spectra of the Au sample resemble those of the Au foil, respectively. This means that most of Au ions in the reaction solution have been reduced to form the Au NCs at the end, in good agreement with that reported by Harada et al. and Bus et al.[24,26]

To investigate the initial kinetics of forming the Au NCs, we further examine the peak C of Au−Au bond produced in the nucleation process. As described before, it is generally assumed that the Au_n^0 clusters are formed first via the Path 1. Then, one may image that the Au−Au bonds observed in the starting nucleation should arise from the Au_n^0 clusters. Seen from the 30 min TEM image, the formed Au_n^0 clusters within the first 60 min are smaller than 1 nm in size, with the number of atoms less than 50. For a small Au NCs with the size of 1.6 nm, Zhang and Sham have reported the bond length contraction (1.4%) of the first shell of the Au−Au bonds with respect to the reference standard of the Au foil.[23] For the small naked Au_n^0 clusters ($n = 2-10$), Wang et al.'s calculation results have indicated that the bond length of Au−Au bonds is in the range of 2.55−2.70 Å, significantly shorter than that (2.87 Å) of the fcc structural Au foil.[27] However, in our case, the position of the peak C for the Au−Au bond as shown in Figure 2e is slightly larger than that of Au foil, which is totally different with the previous results. The succeeding quantitative fitting results of Au−Au bond length as shown later also give the evidence of the expansion of the Au−Au bond length at the initial stage compared with that for bulk Au. Both the qualitative analysis and quantitative fitting results give us an important clue that the formed Au−Au bond does not originate from the small naked Au_n^0 clusters.

To further confirm this point, we performed the XANES calculations (solid lines) for the representative Au_3, Au_{13}, and Au_{43} clusters (Figure 2f), using the *ab initio* multiple-scattering FEFF8.20 code.[28] For comparison, the XANES spectra of $Cl_3^-Au-AuCl_3^-$ dimer cluster and the $HAuCl_4$ aqueous solution are also simulated. To optimize the configuration of the dimer, we also performed the first principles calculations using Gaussian 03 program (see more details in the Supporting Information), and found that the $AuCl_3^-$ is more energetically stable in planar geometry than in tetrahedral configuration. Also, for the calculation of stable configuration of dimer, it was found that tetrahedral complex would be transferred into the planar complex in the optimization process of Gaussian program, that is, every $AuCl_3^-$ unit in the dimer structure is favored in planar geometry. Therefore, the planar−dimer complex is more stable than tetrahedral−dimer complex. The Au−Au and Au−Cl bond distances used in the calculation were selected from the fitting results. The structural model for the higher clusters, such as Au_{13} and Au_{43}, were adopted from the most stable configurations which could be found in ref 26. One can see clearly that the calculated XANES spectra of Au_n^0 clusters do not exhibit any characteristic peaks like the experimental ones measured by *in situ* XAFS. The experimental spectra during the first 60 min, for example, the spectrum of 40 min, are more close to that of dimer configuration, and thus can be well fitted (closed squares) by a linear combination of the spectra of the initial state ($HAuCl_4$ solution) and intermediate state ('Au_2Cl_6' dimers). The proportion of the dimers at this time is about 20%. This means that the Au−Au pairs arise from the complex composed of partially reduced Au ions, indicating the nucleation of Au NCs through Path 2. Once the $AuCl_4^-$ is reduced through the loss of Cl^-, the reduced Au ions would possibly form an Au_nCl_{n+x} complex cluster via the Au−Au bond.

The above discussions lead us to believe that the peaks B and C are most likely related to the partial reduction of Au ions, and the expansion of Au−Au bond length can be attributed to the effect of surrounding Cl^- ions. Similar phenomenon of forming noble metal dimer has been predicted by Ciacchi et al.[15] On the basis of molecular dynamics simulations, they showed that the Pt dimers could be stabilized by Cl^- preferably, and the formation of zerovalent metal clusters is not thermodynamically favored in solutions. Like our results, their simulated bond length (2.90 Å) of Pt−Pt is also larger than that (2.75 Å) of Pt foil. On the other hand, from the viewpoint of reaction condition, Path 2 is more favored under the moderate reduction condition adopted here. For example, in the $PtCl_4^{2-}$ reduction in the presence of a moderate reductant citrate, Henglein et al.[14] have ruled out the existence of Pt^0 atoms but postulated the monovalent Pt dimer as the first reaction intermediates. If in case of strong reducing agents, it has been indicated that the nucleation starts from the full reduction of precursor ions and then the metal clusters are formed.[13] Analogously, it is reasonable to conclude that, under moderate reduction conditions, some kind of Au complex clusters could be formed in the initial nucleation stage prior to the complete reduction of the Au^{3+} ions to zerovalent Au atoms.

To obtain quantitative structural parameters around Au atoms in reaction process, a least-squares curve parameter fitting was performed using the ARTEMIS module of IFEFFIT and USTCXAFS software packages.[29,30] In the curve-fitting analysis, the peaks in the range of 1.2−3.4 Å were attributed to Au−Cl and Au−Au bonds without any contribution of the Au−O bond, which coincides with the fitting strategy used in the references.[24,31] The curve-fitting results for the samples at typical reaction times are displayed in Figure S3. The obtained coordination number (N) and bond distance (R) are shown in Figure 3 against time. The N_{Au-Cl} (Figure 3c) was found to be around 4 in the absence of the reducing agent and decreased to 3 at about 30 min, indicating the reduction of Au^{3+} ($AuCl_4^-$) to Au^{2+} ($AuCl_3^-$) species.[18,32] At the same time, the N_{Au-Au} is almost equal to 1. Thus, this suggests the formation of the $Cl_3^-Au-AuCl_3^-$ ('Au_2Cl_6') dimers from two reduced $AuCl_3^-$ at first. Then, these minuscule Au_2Cl_6 clusters could be further reduced and aggregated to form larger Au_nCl_{n+x} complex clusters consisting of several Au atoms in the early stage. The reaction of other Au ions species with the clusters is expected to occur preferentially via electron transfer from the reductant to these dimeric and trimeric units.[33] Therefore, with the reduction continued, the higher polymers are evolved on the basis of these dimers and trimers. Additionally, the Au−Au bond length evaluated by EXAFS fitting analysis at the beginning of the formation of

(26) Bus, E.; Prins, R.; van Bokhoven, J. A. *Phys. Chem. Chem. Phys.* **2007**, *9*, 3312.
(27) Wang, J. L.; Wang, G. H.; Zhao, J. J. *Phys. Rev. B* **2002**, *66*, 035418.
(28) Ankudinov, A. L.; Bouldin, C. E.; Rehr, J. J.; Sims, J.; Hung, H. *Phys. Rev. B* **2002**, *65*, 104107.
(29) Ravel, B.; Newville, M. *J. Synchrotron Radiat.* **2005**, *12*, 537.
(30) Zhong, W. J.; He, B.; li, Z.; Wei, S. Q. *J. China Univ. Sci. Technol.* **2001**, *31*, 328.
(31) Yu, K.; Yao, T.; Pan, Z. Y.; Wei, S. Q.; Xie, Y. *Dalton Trans.* **2009**, *46*, 10353.
(32) Tsai, Y. W.; Tseng, Y. L.; Sarma, L. S.; Liu, D. G.; Lee, J. F.; Hwang, B. J. *J. Phys. Chem. B* **2004**, *108*, 8148.
(33) *Clusters and Colloids: From Theory to Applications*; Schmid, G. , Ed.; VCH: Weinheim, 1994.

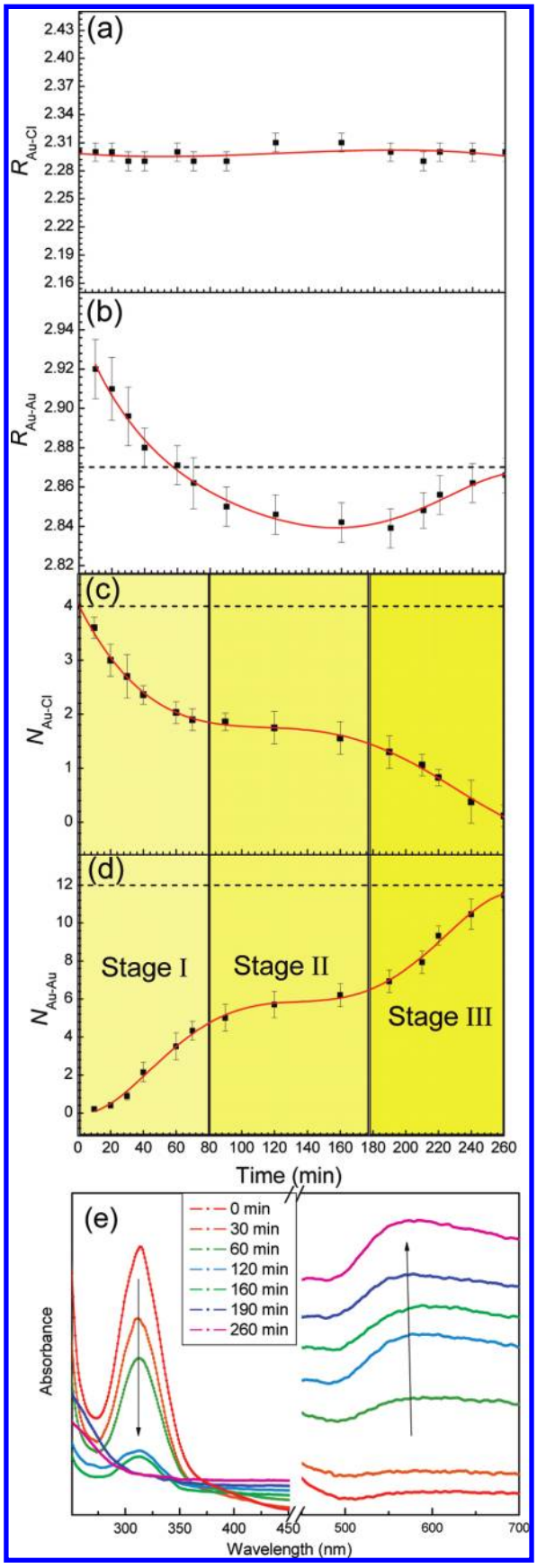

Figure 3. Time profiles of various structural parameters from the EXAFS fitting: The bond distance for Au−Cl (a) and Au−Au (b) bonds. The coordination number for Au−Cl (c) and Au−Au (d) bonds. The dashed lines are noted as the corresponding values of reference $HAuCl_4$ and bulk Au. (e) Temporal evolution of UV−vis absorption spectra of the Au colloidal solutions.

Au−Au bond is 2.92 Å, which is 1.7% larger than the corresponding value (2.87 Å) for bulk Au. For these 'Au_2Cl_6' clusters formed in the early stage, Au ions are almost enclosed by Cl ions. The charge transfer between Au and Cl atoms would thus overcome nanosize effects and lead to the expansion of the Au−Au bond length in the Au complex clusters as revealed by the Figure 2e. Moreover, because the number of Au atoms in clusters increases with the reaction time, the specific surface area per Au atom and the Cl^- capping efficiency are therefore lowered. The competition between size and ligand effects tunes the R_{Au-Au} smaller than that of bulk gold for Au NCs larger than 9 nm, which can be seen from the trend in Figure 3b.

Furthermore, according to the temporal evolutions of N_{Au-Cl} and N_{Au-Au} shown in Figure 3c,d, we can classify the whole reaction into three stages, that is, stage I, II, and III as marked by the highlight. Stage I can be considered as the initial nucleation step, exhibiting a faster process compared with stage II which stands for the growth step. In stage III, however, N_{Au-Au} increases quickly along with the decreased N_{Au-Cl}, indicating the rapid increase in size of Au NCs. This three-step mechanism can also be supported with a time evolution of UV−vis absorption spectra shown in Figure 3e. Within the first 80 min (stage I), the intensity of the absorbance at 327 nm from the gold salt in $AuCl_4^-$ rapidly decreases, while the surface plasmon resonance (SPR) peak of Au colloid gradually appears, corresponding to the nucleation stage. In the middle stage from 120 to 180 min (stage II), these two peaks show little variations, and finally in stage III, pronounced SPR peaks can be observed.

Summarizing the above results, we present a possible schematic pathway to illustrate the initial nucleation and growth kinetics of Au NCs in Figure 4. In the early nucleation (stage I), two dispersed $AuCl_3^-$ ions were first connected via the Au−Au pair with the bond length significantly larger than that of the bulk Au, yielding the $Cl_3^-Au-AuCl_3^-$ dimers which could then react with an $AuCl_4^-$ ion to form trimers. Analogously, the higher polymers and small Au clusters (such as Au_{13} cluster) could be formed in the subsequent reduction (stage II). In these clusters, the Au atoms are mostly coordinated with other Au atoms, resulting in much larger N_{Au-Au} than in dimers or trimers. Then, the formation of small Au NCs could be observed by TEM, which showed the appearance of 2.5 nm NCs, corresponding to the N_{Au-Au} of about 7 at the reaction time of 120 min. The structural transition from two-dimensional (2D) to three-dimensional (3D) of Au clusters has been predicted by theoretical calculations.[27,34] Wang et al.[27] and Madsen et al.[34] have suggested that this transition occurs at the critical atomic number of about 7. When the number of Au atoms in a complex cluster exceeds the critical value of 13−15, fcc structured Au NCs are developed.[35] Therefore, the fast nucleation might be due to the fact that Au atoms are nearly all surface atoms and have high surface energy for Au_nCl_{n+x} complex clusters with $n \leq 7$. However, the growth kinetics could in principle be slowed by the steric hindrance of the ligands such as PVP.[31,36] For the larger 'Au_iCl_j' clusters with Cl^- ions surrounding on the surface, which are further stabilized by the capping agent of citric acid together with the PVP protection, the proportion of active sites located at the surface is decreased. Hence, the transition to 3D structure and then the formation of fcc Au NCs occurring at the beginning of stage II lead to the slow growth as witnessed

(34) Ferrighi, L.; Hammer, B.; Madsen, G. K. H. *J. Am. Chem. Soc.* **2009**, *131*, 10605.
(35) Hakkinen, H. *Chem. Soc. Rev.* **2008**, *37*, 1847.
(36) Sau, T. K.; Murphy, C. J. *J. Am. Chem. Soc.* **2004**, *126*, 8648.

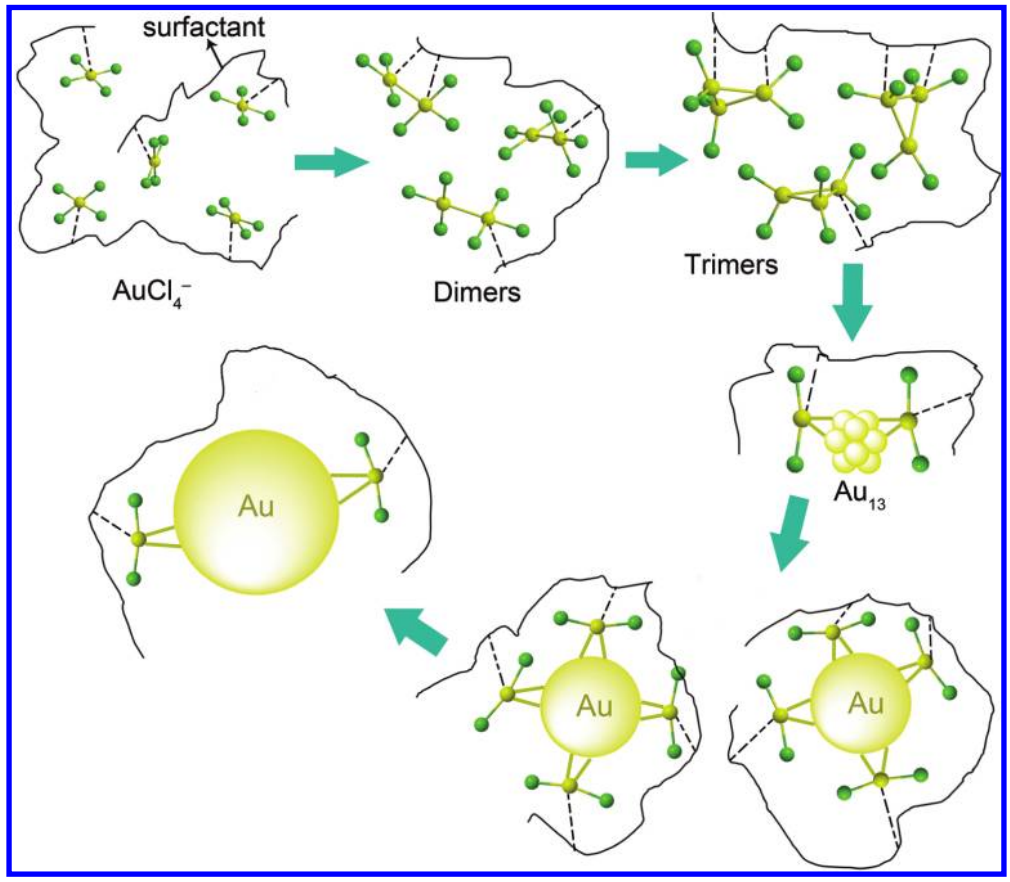

Figure 4. A schematic representation of the formation process of Au NCs. The ruleless line represents the surfactant. At first, the $AuCl_4^-$ ions are dispersed in the colloidal solution. Then, the dimers and trimers are formed which can be classified into the stage I. For the small Au clusters in the stage II, the representative Au_{13} cluster is shown. Finally, the large Au NCs are produced (stage III).

by the 'plateau' in Figure 3d. Finally, the larger Au NCs with stable size were produced. The significant accelerating of growth rate (stage III) after the accumulatively mild reaction may be attributed to the coalescence of individual particles. Considering that the nuclei serve as the foundation for the NCs growth, the 'Au_nCl_{n+x}' clustering structure proposed here plays an important role in directing the later growth. Controlling the initially formed complex clusters may provide an effective mean to obtain the shape-controllable nanocrystals.

Conclusions

Using continuous-flow *in situ* XAFS spectroscopy, we have determined the initial nucleation kinetics of Au NCs reduced from the $AuCl_4^-$ in the aqueous solution. The analysis of XAFS indicates that, in the moderate reaction condition, the partially reduced $AuCl_3^-$ ions would be combined through the slightly elongated Au−Au bond to form the Au_nCl_{n+x} complex clusters rather than to form Au_n^0 clusters. These complex clusters play an important role in delaying the following growth and inducing the eventual coalescence. These findings enrich our understanding of the nucleation process of nanocluster formation, and the *in situ* XAFS spectroscopic method could be broadly applicable to the study of the kinetics of chemical liquid phase syntheses of other transition-metal NCs. Furthermore, since the nucleation process has scientific importance in directing the nanocrystal formation, it is expected that the understanding of the nucleation mechanism can guide the way toward the design and synthesis of nanomaterials in a controllable manner.

Acknowledgment. This work was supported by the National Natural Science Foundation of China (Grant Nos. 10635060, 10725522, 10979047, 10605024, and 20701036) and the National Basic Research Program of China (No. 2009CB939901). The authors would like to thank KEK-PF and NSRL for access to facilities and for the funding that permitted the development of this experiment.

Supporting Information Available: Additional details on the procedures of nanocrystals synthesis as well as the measurements of TEM, UV−vis and XAFS. Supporting results mentioned in the text, including Figures S1−S3. This material is available free of charge via the Internet at http://pubs.acs.org.

JA101101D